Interaction with surrounding normal epithelial cells influences signalling pathways and behaviour of Src-transformed cells

Mihoko Kajita[1], Catherine Hogan[1], Andrew R. Harris[2], Sophie Dupre-Crochet[1,*], Nobue Itasaki[3], Koichi Kawakami[4], Guillaume Charras[2,5], Masazumi Tada[5] and Yasuyuki Fujita[1,5,‡]

[1]MRC Laboratory for Molecular Cell Biology and Cell Biology Unit and [5]Department of Cell and Developmental Biology, University College London, London, WC1E 6BT, UK
[2]London Centre for Nanotechnology, London, WC1H 0AH, UK
[3]Division of Developmental Neurobiology, National Institute for Medical Research, London, NW7 1AA, UK
[4]Division of Molecular and Developmental Biology, National Institute of Genetics and Department of Genetics, The Graduate University for Advanced Studies (SOKENDAI), Mishima, Shizuoka 411-8540, Japan
*Present address: INSERM UMR 757, Université Paris-sud, Bat 443, 91405 Orsay cedex, France
‡Author for correspondence (y.fujita@ucl.ac.uk)

Accepted 2 November 2009
Journal of Cell Science 123, 171-180 Published by The Company of Biologists 2010
doi:10.1242/jcs.057976

Summary

At the initial stage of carcinogenesis, transformation occurs in a single cell within an epithelial sheet. However, it remains unknown what happens at the boundary between normal and transformed cells. Using Madin-Darby canine kidney (MDCK) cells transformed with temperature-sensitive v-Src, we have examined the interface between normal and Src-transformed epithelial cells. We show that Src-transformed cells are apically extruded when surrounded by normal cells, but not when Src cells alone are cultured, suggesting that apical extrusion occurs in a cell-context-dependent manner. We also observe apical extrusion of Src-transformed cells in the enveloping layer of zebrafish gastrula embryos. When Src-transformed MDCK cells are surrounded by normal MDCK cells, myosin-II and focal adhesion kinase (FAK) are activated in Src cells, which further activate downstream mitogen-activated protein kinase (MAPK). Importantly, activation of these signalling pathways depends on the presence of surrounding normal cells and plays a crucial role in apical extrusion of Src cells. Collectively, these results indicate that interaction with surrounding normal epithelial cells influences the signalling pathways and behaviour of Src-transformed cells.

Key words: Apical extrusion, Focal adhesion kinase, Mitogen-activated protein kinase, Myosin-II, Src, Zebrafish

Introduction

In most epithelial tissues, cells are connected to each other via tight cell-cell contacts, forming a continuous monolayer. These epithelial cells receive a variety of signals, including those transmitted via cell-cell adhesions, which control their proliferation, differentiation, movement and survival (Fagotto and Gumbiner, 1996; Jamora and Fuchs, 2002). Cell transformation occurs through the activation of proto-oncoproteins and the inactivation of tumour suppressor proteins (Hanahan and Weinberg, 2000). In the initial step of carcinogenesis, transformation occurs in a single cell within an epithelial sheet (Fialkow, 1976; Nowell, 1976). However, it is not clear what happens at the interface between transformed and surrounding normal cells. Do normal and transformed cells recognize the differences between them? If so, how do they respond to these differences?

These questions have been addressed in the epithelium of imaginal discs in *Drosophila* embryos (Baker and Li, 2008; Diaz and Moreno, 2005). For example, when wild-type and Myc-overexpressing cells coexist in the epithelium, the wild-type cells surrounding the Myc-overexpressing cells undergo apoptosis (de la Cova et al., 2004; Moreno and Basler, 2004). When *scribble*-deficient cells are surrounded by wild-type cells, the *scribble*-deficient cells undergo apoptosis and are eliminated from the epithelium (Brumby and Richardson, 2003). When Src-activated (Csk-knockdown) cells are surrounded by wild-type cells, the Src-activated cells are basally extruded and then die by apoptosis (Vidal et al., 2006). Importantly, these processes of cell death and extrusion occur only when wild-type and transformed cells contact one another in an epithelial monolayer. The molecular mechanisms involved are largely unknown.

We have recently reported the events occurring at the interface between normal and RasV12-transformed epithelial cells using a mammalian cell culture system (Hogan et al., 2009). When RasV12-expressing MDCK cells are surrounded by normal MDCK cells, the RasV12 cells are either apically extruded from the monolayer, or form dynamic basal protrusions and invade the basal matrix. These observations suggest that the RasV12 cells recognize a difference in the surrounding normal cells and leave the epithelial sheet either apically or basally, depending on the cell context. However, it remains unknown whether transformation with other oncoproteins causes comparable phenomena in vertebrates.

The Rous sarcoma virus *src* gene (*v-src*) was the first identified oncogene (Hunter and Sefton, 1980). v-Src and its cellular counterpart c-Src are non-receptor tyrosine kinases that phosphorylate multiple proteins on tyrosines and thereby regulate actin cytoskeleton, cell adhesions, cell proliferation and other cellular processes (Frame, 2002; Frame et al., 2002; Parsons and Parsons, 2004). In this study, using MDCK cells expressing a temperature-sensitive v-Src mutant, we have examined the interface between normal and Src-transformed epithelial cells.

Results

Src-transformed cells are apically extruded from a monolayer of normal epithelial cells

To investigate the phenomena occurring at the interface between normal and transformed epithelial cells, we have used MDCK cells transformed with a temperature-sensitive v-Src mutant (ts-Src MDCK cells). At 40.5°C (the non-permissive temperature for ts-Src activity), cells formed tight intercellular adhesions and exhibited the characteristic cobble-stone morphology of untransfected MDCK cells (Behrens et al., 1993; Fujita et al., 2002). After a temperature shift to 35°C (the permissive temperature for ts-Src activity), the activity of ts-Src started to increase at 10 minutes and reached a maximum at 1-2 hours (Behrens et al., 1993; Woodcock et al., 2009). When cells were plated at low density, a temperature shift to 35°C induced cell scattering and downregulation of cell-cell contacts (Behrens et al., 1993; Fujita et al., 2002). By contrast, when cells were plated at high density, a temperature shift did not induce loss of cell-cell contacts, and cells retained an epithelial morphology (Fig. 1B). In all subsequent experiments, we cultured cells at high density.

To examine the fate of Src-transformed MDCK cells in a monolayer of untransformed MDCK cells, we labelled ts-Src MDCK cells with a fluorescent dye (CMTPX) and mixed them with untransfected (normal) MDCK cells at a ratio of 1:100. The mixture of cells was then cultured on a collagen matrix and incubated at 40.5°C until a monolayer was formed. Subsequently, activation of ts-Src was induced by a temperature shift to 35°C, and the fate of ts-Src MDCK cells surrounded by normal MDCK cells was observed using time-lapse microscopy. Between 12 and 24 hours after the temperature shift, we observed that Src cells were frequently extruded from the apical surface of the monolayer (80%, n=90) (Fig. 1A,C,D; supplementary material Fig. S1A,B and

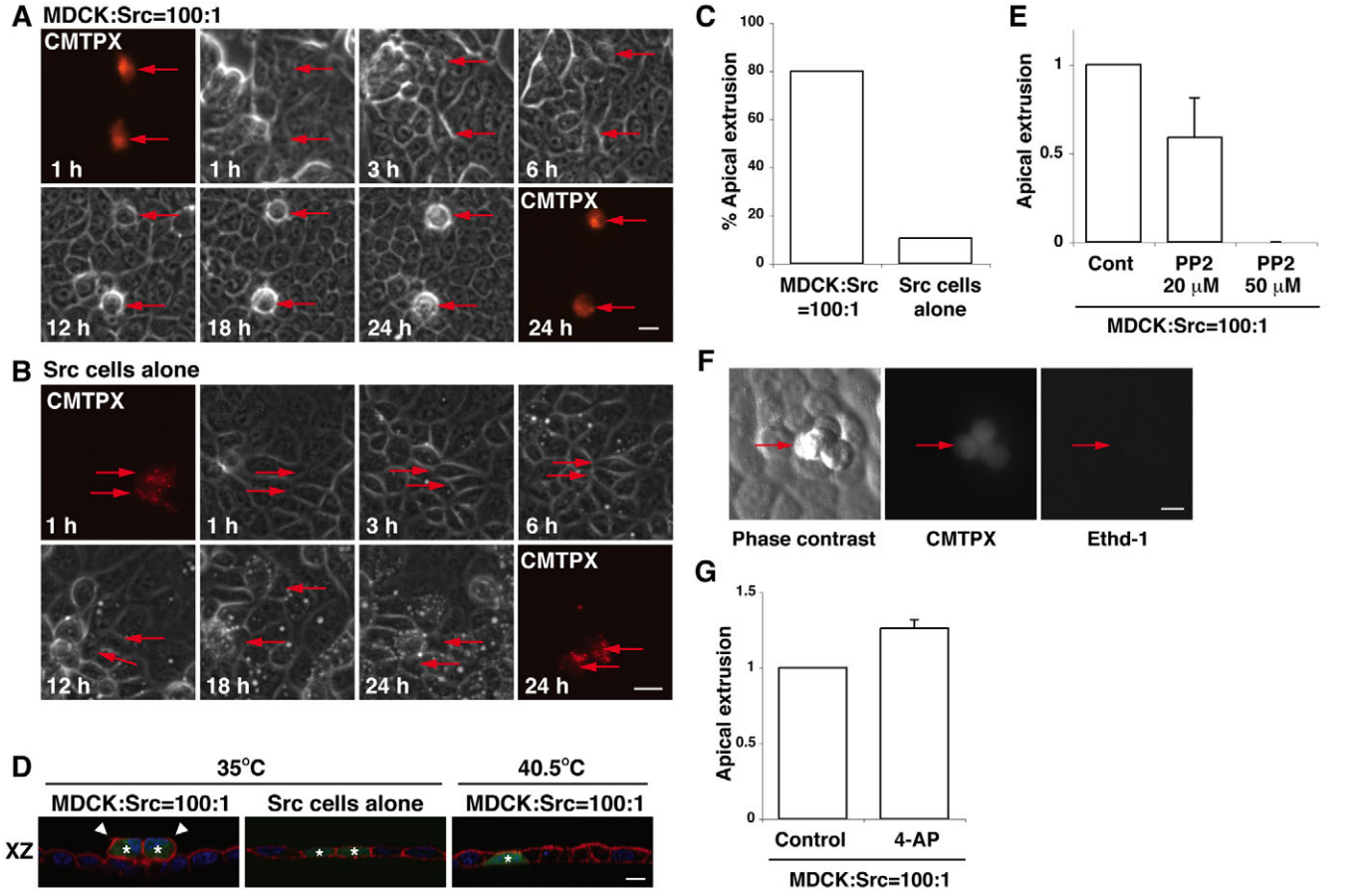

Fig. 1. Src-transformed cells are apically extruded from a monolayer of normal epithelial cells in a cell death-independent manner. (**A**,**B**) ts-Src MDCK cells are apically extruded when they are surrounded by normal MDCK cells, but not when surrounded by ts-Src MDCK cells. ts-Src MDCK cells were stained with a fluorescent dye (CMTPX, red) and mixed with normal MDCK cells (A) or ts-Src MDCK cells (B), followed by a temperature shift (35°C). Images are extracted from a representative time-lapse analysis. Red arrows indicate fluorescently labelled Src cells. (**C**) Quantification of time-lapse analyses of ts-Src MDCK cells extruded from a monolayer of normal MDCK cells or from that of ts-Src MDCK cells within 24 hours after the temperature shift (n=90 for the former and n=72 for the latter from 4-5 independent experiments). (**D**) Immunofluorescence images of XZ sections of ts-Src MDCK cells (stained with CMFDA, green) that are surrounded by normal MDCK cells (left and right panels) or by ts-Src MDCK cells (middle panel). Cells were cultured at 35°C or 40.5°C for 24 hours, and were stained with phalloidin (red) and Hoechst 33342 (blue). Asterisks and arrowheads indicate fluorescently labelled Src cells and extruded Src cells, respectively. (**E**) Quantification of apical extrusion of Src cells in the absence or presence of PP2. (**F**) Extruded ts-Src MDCK cells remain alive on a monolayer of normal MDCK cells. The mixture of normal and Src cells were stained with ethidium homodimer-1 (Ethd-1) for 8 hours after 16 hours of the temperature shift. Red arrows indicate extruded Src cells. (**G**) Quantification of apical extrusion of Src cells in the absence or presence of 4-AP. Values in E and G are expressed as a ratio relative to control. Data are mean ± s.d. from three (E) or two (G) independent experiments. Scale bars: 20 μm (A,B) or 10 μm (D,F).

Movies 1, 2). The extrusion often occurred in single Src cells (Fig. 1A), but a group of two to four Src cells were also extruded (Fig. 1D,F; supplementary material Fig. S1A,B). Addition of the Src inhibitor PP2 strongly suppressed apical extrusion of Src cells (Fig. 1E). At 40.5°C, the extrusion of Src cells from a monolayer of normal cells did not occur (Fig. 1D). Furthermore, at 35°C, Src cells were not apically extruded from a monolayer of only Src cells (Fig. 1B-D; supplementary material Movie 3). Collectively, these data indicate that both Src activation and the presence of surrounding normal cells are required for the apical extrusion of Src cells. The extruded Src cells did not stain with a membrane-impermeable ethidium dye (Fig. 1F), indicating that their plasma membrane was still intact. Treatment with the K^+ channel inhibitor 4-aminopyridine (4-AP), which blocks apoptosis of MDCK cells at a very early stage (Rosenblatt et al., 2001), did not significantly suppress apical extrusion (Fig. 1G), suggesting that extrusion occurred in an apoptosis-independent manner.

Previously, we reported that when RasV12-expressing MDCK cells are surrounded by normal MDCK cells, the RasV12 cells are apically extruded from the monolayer, or form dynamic basal protrusions and invade the basal matrix (Hogan et al., 2009). To examine the involvement of Ras signalling pathways in apical extrusion of Src cells, we used a transient transfection method. The transfection efficiency is very low in MDCK cells, thus a transient transfection method induces the condition under which a small number of transfected cells are surrounded by the majority of untransfected cells. First, we confirmed that transient transfection of MDCK cells with v-Src induced apical extrusion of v-Src-expressing cells that were surrounded by untransfected cells, comparable to that observed in ts-Src MDCK cells (supplementary material Fig. S2A). Using this method, we found that coexpression of dominant-negative Ras significantly suppressed apical extrusion of v-Src-expressing cells (supplementary material Fig. S2B). Moreover, we also found that addition of the Src inhibitor PP2 significantly suppressed apical extrusion of RasV12-transformed cells that were surrounded by normal cells (supplementary material Fig. S2C). These data suggest that Ras and Src pathways play a role in apical extrusion of Src- and Ras-transformed cells, respectively, and that some common molecular mechanisms are probably involved in these processes. However, Ras-transformed cells that were not apically extruded formed basal protrusions (Hogan et al., 2009), whereas Src-transformed cells did not form similar protrusions (supplementary material Fig. S3), suggesting that distinct signalling pathways are also regulated at the interface between normal and respective transformed cells (please see further comparisons in Discussion).

Next, we analysed ts-Src MDCK cells that were surrounded by normal MDCK cells but were not yet extruded from the monolayer. We observed that the height of Src cells along the apicobasal axis was significantly greater than that of the surrounding normal cells (Fig. 2A,C). In addition, the Src cells had a round shape rather than a cuboidal shape (Fig. 2A). Src cells within a monolayer of only Src cells did not show these changes in cell height or shape (Fig. 2B,C). These results suggest that Src cells recognize that they are surrounded by normal cells and change their morphology accordingly.

Furthermore, we examined whether apical extrusion of Src-activated cells occurs in vivo using zebrafish embryos. During zebrafish gastrulation, embryonic deep cells are enwrapped by the enveloping layer (EVL), an outermost epithelial monolayer (Carreira-Barbosa et al., 2009; Koppen et al., 2006). Using an EVL-specific Gal4-driver line in combination with injection of a UAS-vector carrying v-Src (Fig. 3A,B), we expressed v-Src specifically within the EVL in a mosaic manner and analysed the fate of these v-Src-expressing cells. We observed that the v-Src-expressing cells were frequently extruded from the apical surface of the epithelial monolayer (Fig. 3D,E; arrows). We also found that the height of v-Src-expressing cells that remained in the monolayer was often increased compared to that of their non-Src-expressing neighbours (Fig. 3C-E; arrowheads). The shape of the nucleus in these v-Src-expressing cells remained normal (Fig. 3D,E), suggesting that the observed phenomena were not caused by a toxic effect of v-Src expression. Cells expressing a control vector did not change their height and were not extruded (Fig. 3C,D). These data indicate that apical extrusion of Src-transformed cells indeed occurs in vivo.

Myosin-II and MAPK are involved in apical extrusion of Src-transformed cells

To elucidate the molecular mechanisms involved in apical extrusion, we examined the effect of various inhibitors. We tested Blebbistatin,

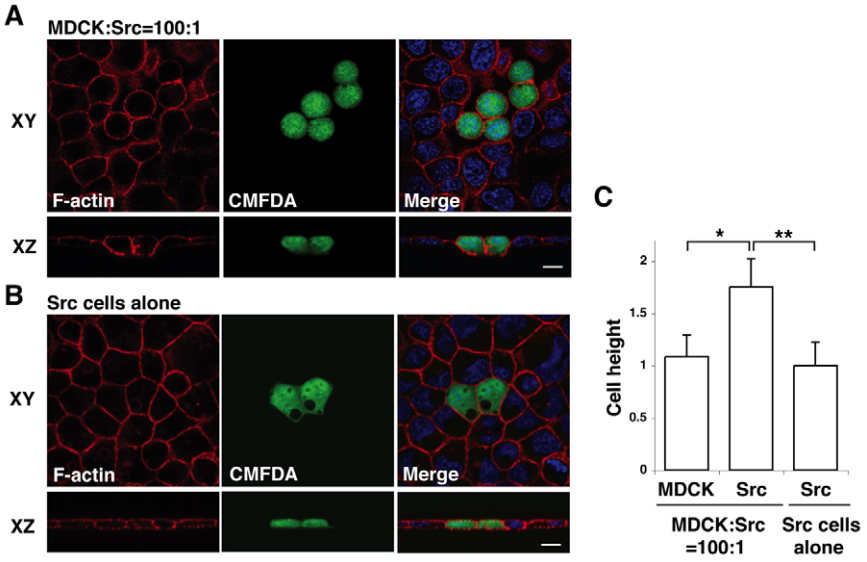

Fig. 2. Morphological changes of Src-transformed cells that are surrounded by normal epithelial cells. (**A**,**B**) Immunofluorescence images of ts-Src MDCK cells (stained with CMFDA, green) that are surrounded by normal MDCK cells (A) or by ts-Src MDCK cells (B). Cells were stained with phalloidin (red) and Hoechst 33342 (blue) after 16 hours of the temperature shift. Scale bars; 10 μm. (**C**) Quantification of cell height. Data are mean ± s.d. $*P<5\times10^{-23}$, $**P<2\times10^{-24}$; n=46, 48 and 53 cells from three independent experiments. Values are expressed as a ratio relative to Src cells alone.

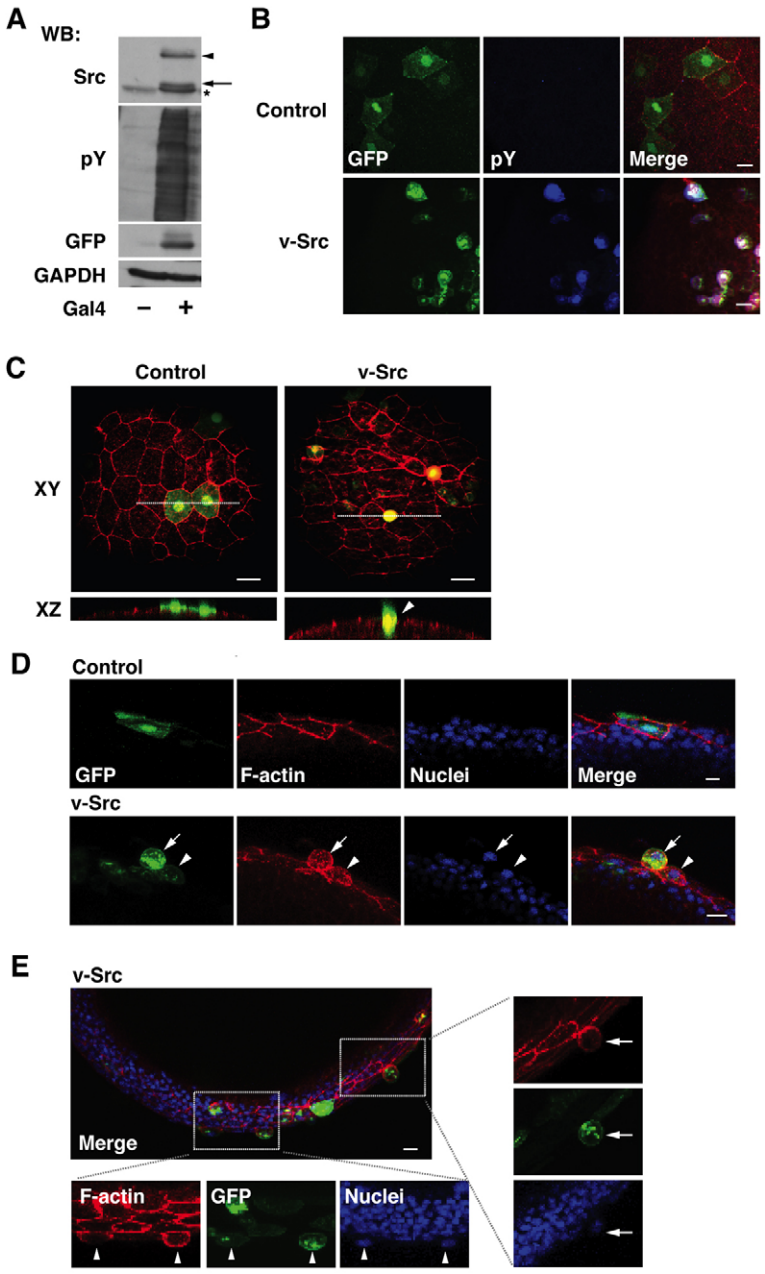

Fig. 3. v-Src-expressing cells are apically extruded from a monolayer of the enveloping layer (EVL) in zebrafish embryos. (**A**) Gal4-dependent expression of v-Src. pBR-Tol2-UAS-GAP43-GFP-SC-v-Src was transfected without or with pCS2-Gal4FF in HEK293 cells. Cell lysates were examined by western blotting using anti-Src, anti-phospho-tyrosine (pY), and anti-GFP antibodies. Equal protein loading was confirmed using anti-GAPDH antibody. In this system, the expressed proteins (GAP43-GFP-SC-v-Src) were cleaved at the self-cleaving peptide sequence (SC), leading to expression of GAP43-GFP and v-Src. Arrowhead and arrow indicate non-cleaved GAP43-GFP-SC-v-Src and cleaved v-Src, respectively. The asterisk indicates endogenous c-Src. (**B**) Immunofluorescence images of embryos at 9 hours post-fertilization (hpf) (90% epiboly), injected with the control (upper panels) or v-Src-expressing vector (lower panels) at the one- to two-cell stage. Embryos were stained with phalloidin (red) and anti-pY antibody (blue). (**C-E**) Immunofluorescence images of zebrafish embryos (at 8-9 hpf), injected with the control or v-Src-expressing vector at the one- to two-cell stage. Embryos were stained with phalloidin (red) and/or Hoechst 33342 (blue). Surface views (C) and semi-lateral views (D,E) of embryos. (C) White dotted lines in XY panels denote cross-section represented in XZ sections. (E) The areas in the white box are shown in higher magnification. (C-E) Arrowheads and arrows indicate v-Src-expressing cells with increased cell height and extruded v-Src-expressing cells, respectively. Representative images are shown from 18 and 30 embryos that were injected with the control or v-Src-expressing vector respectively, from three independent experiments. Scale bars: 20 μm (B), 40 μm (C) and 10 μm (D,E).

an inhibitor of myosin-II, because myosin-II has been reported to regulate cell morphology by modulating the actin cytoskeleton (Krendel and Mooseker, 2005; Lecuit and Lenne, 2007; Quintin et al., 2008). As shown in Fig. 4, Blebbistatin strongly suppressed apical extrusion of ts-Src MDCK cells from a monolayer of normal MDCK cells. The activity of myosin-II is regulated by both myosin light chain kinase (MLCK) and Rho kinase (ROCK) through the phosphorylation of myosin light chain (MLC) (Ikebe and Hartshorne, 1985; Kimura et al., 1996). ML-7 and Y27632, which inhibit MLCK and ROCK respectively, significantly suppressed apical extrusion (Fig. 4), suggesting that both kinases are at least partially involved in this process. Furthermore, U0126, an inhibitor of MEK (MAP kinase kinase), substantially blocked apical extrusion, whereas the phosphoinositide 3-kinase (PI3K) inhibitor LY294002 or the Gap junction inhibitor 18-α-glycyrrhetinic acid (αGA) had no effect (Fig. 4). Collectively, these results suggest that myosin-II and MAPK pathways play crucial roles in apical extrusion of Src cells.

To understand whether myosin-II activity is required in the Src cells and/or neighbouring normal cells, we analysed the activity of myosin-II by immunofluorescence. When ts-Src MDCK cells alone formed a monolayer, phosphorylation of MLC was observed at basal and basolateral plasma membrane domains and was significantly greater than that observed in normal MDCK cells (Fig. 5A,B). Interestingly, when Src cells were surrounded by normal cells, phosphorylation of MLC in the Src cells was further enhanced around the whole cortical region of the plasma membrane (Fig. 5A,B), raising the possibility that myosin-II activity in the Src cells is required for their extrusion. To test this possibility directly, we used a transient transfection method. We found that coexpression of dominant-negative MLC (MLC-AA) significantly suppressed the

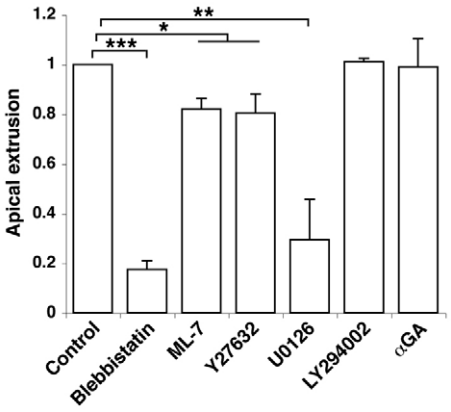

Fig. 4. Quantification of apical extrusion of Src cells with various inhibitors. ts-Src MDCK cells were cultured with normal MDCK cells in the presence of various inhibitors, and apical extrusions of the Src cells were analysed after 24 hours of the temperature shift. Data are mean ± s.d. from three independent experiments for Blebbistatin, Y27632 and U0126, or from two independent experiment for ML-7, LY294002, and αGA. **P*<0.03, ***P*<0.002, ****P*<0.0002. Values are expressed as a ratio relative to control.

apical extrusion of v-Src-expressing cells (supplementary material Fig. S4), suggesting that activity of myosin-II in the Src cells plays a role in apical extrusion.

We also analysed the activity of MAPK in ts-Src MDCK cells by immunofluorescence. When Src cells alone were cultured, phosphorylation of MAPK was mainly observed at cell-cell contact sites, and the fluorescence intensity was greater than that in normal cells (Fig. 5C,D). When Src cells were surrounded by normal cells, phosphorylation of MAPK in the Src cells was further enhanced and was observed around the entire plasma membrane (Fig. 5C,D). These data demonstrate that myosin-II and MAPK activities are upregulated in Src cells that are surrounded by normal cells.

To understand the relationship between these two activities, we examined the effects of Blebbistatin or U0126 on the phosphorylation of myosin-II and MAPK in Src cells that were surrounded by normal cells. Whereas the MEK inhibitor U0126 did not affect the phosphorylation of MLC (Fig. 5E), Blebbistatin significantly suppressed the phosphorylation of MAPK (Fig. 5F). These findings suggest that myosin-II functions, at least partially, upstream of MAPK.

The E-cadherin–β-catenin complex localizes to the basal side of cell-cell adhesions of Src cells in a monolayer of normal cells

We next examined the effect of Src activation on E-cadherin-based cell-cell adhesions. When Src cells alone formed a monolayer, β-catenin and E-cadherin colocalized with F-actin along the entire basolateral plasma membrane (Fig. 6A,B; and data not shown). By contrast, when Src cells were surrounded by normal cells, β-catenin

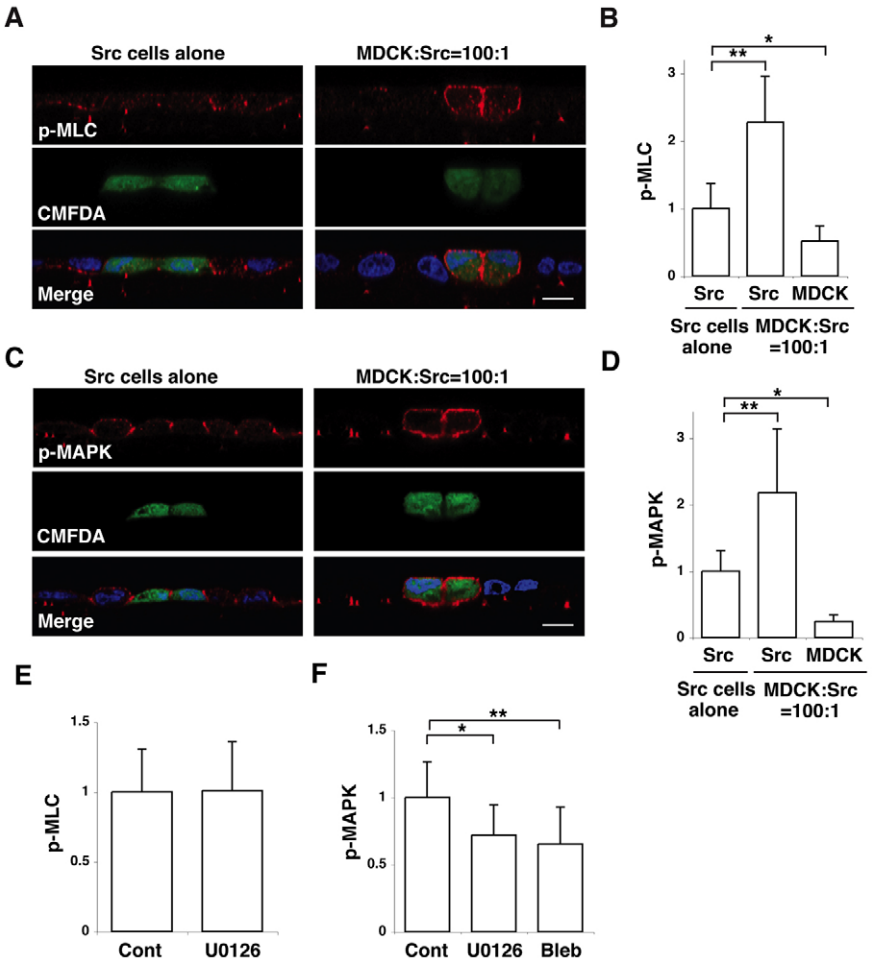

Fig. 5. Activity of myosin-II and MAPK is further enhanced in Src cells when they are surrounded by normal cells. (**A**,**C**) Immunofluorescence images of XZ sections of Src cells (stained with CMFDA, green) surrounded by Src cells (left panels) or by normal MDCK cells (right panels). Cells were stained with Hoechst 33342 (blue) and anti-MLC-*P* (p-MLC) antibody (A, red) or anti-MAPK-*P* (p-MAPK) antibody (C, red). Scale bars; 10 μm. (**B**,**D**) Quantification of immunofluorescence of MLC-*P* (B) or MAPK-*P* (D). Data are mean ± s.d. (B) **P*<4×10^{-7}, ***P*<6×10^{-15}; *n*=38, 37 and 33 cells from three independent experiments. (D) **P*<5×10^{-16}, ***P*<3×10^{-11}; *n*=45, 42 and 23 cells from three independent experiments. (**E**,**F**) Quantification of immunofluorescence of MLC-*P* (E) or MAPK-*P* (F) in Src cells that were cultured with normal MDCK cells in the presence of the indicated inhibitors. It should be noted that Blebbistatin suppresses ATPase activity of myosin-II without affecting the phosphorylation of MLC, thus the effect of Blebbistatin on MLC-*P* was not examined. Data are mean ± s.d. (E) *n*=80 and 62 cells from four independent experiments. (F) **P*<0.0001, Z=4.2; ***P*<0.0001, Z=5.4; *n*=51, 28 and 40 cells from three independent experiments. Values are expressed as a ratio relative to Src cells alone (B,D) or to control (E,F). Two-tailed Student's *t* tests were used to determine *P*-values, except for Fig. 5F where Mann-Whitney *U*-tests were used.

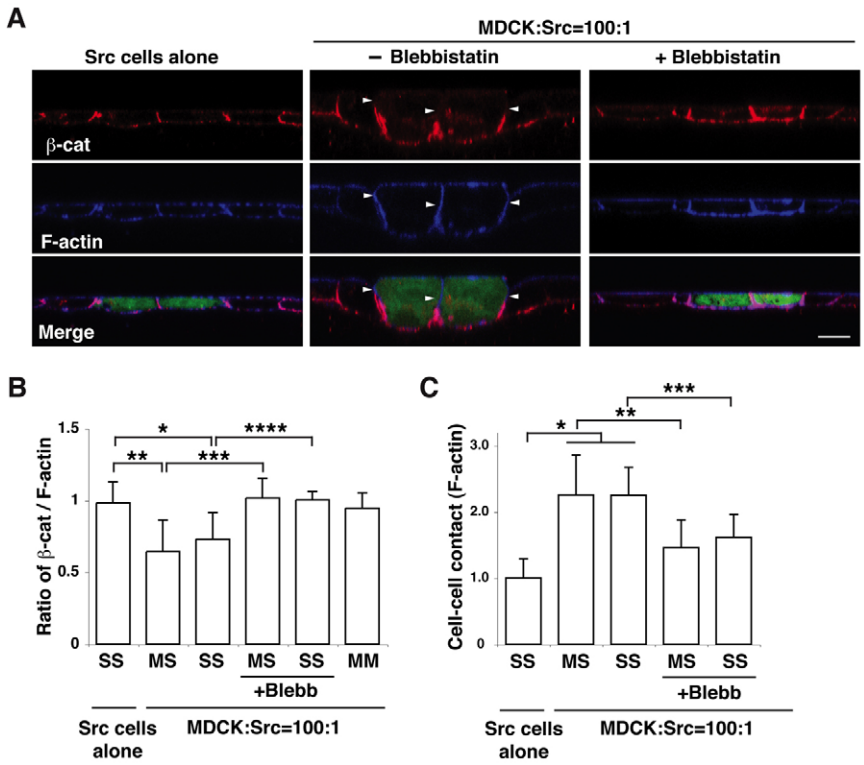

Fig. 6. β-catenin is basally relocalized in Src-transformed cells that are surrounded by normal cells. (**A**) Immunofluorescence of XZ sections of β-catenin and F-actin. ts-Src MDCK cells were stained with CMFDA (green) and cultured with ts-Src MDCK cells (left panels) or with normal MDCK cells (middle and right panels) in the absence or presence of Blebbistatin. Cells were stained with anti-β-catenin antibody (red) and phalloidin (blue). Scale bar: 10 μm. Arrowheads indicate the lateral membrane domain where immunofluorescence of β-catenin is absent but that of F-actin is present. (**B**) Quantification of the length of lateral membrane domains with β-catenin–F-actin fluorescence. The length of basolateral domains stained with β-catenin or F-actin was measured, and the ratio of the length (β-catenin–F-actin) was calculated. MM, between normal MDCK cells; MS, between normal and ts-Src MDCK cells; SS, between ts-Src MDCK cells. Data are mean ± s.d. $*P<4\times10^{-11}$, $**P<4\times10^{-27}$, $***P<9\times10^{-29}$, $****P<8\times10^{-8}$; n=101, 87, 27, 81, 20 and 64 cell-cell contact sites from three independent experiments. (**C**) Quantification of the length of cell-cell contact area. The length of cell-cell contact area stained with F-actin was measured. Data are mean ± s.d. $*P<2\times10^{-28}$, $**P<2\times10^{-17}$, $***P<7\times10^{-6}$; n=84, 78, 19, 80 and 21 cell-cell contact sites from three independent experiments. Values are expressed as a ratio relative to cell-cell contact sites between ts-Src MDCK cells where ts-Src MDCK cells alone are cultured.

and E-cadherin disappeared from the apical side of the cell-cell adhesions between normal and Src cells, as well as between adjacent Src cells, whereas F-actin localization remained at the whole intercellular adhesions (Fig. 6A,B; and data not shown). Addition of Blebbistatin restored the E-cadherin–β-catenin complex along the entire cell-cell contact sites (Fig. 6A,B), whereas addition of U0126 had no observable effect (supplementary material Fig. S5B). Furthermore, we also found that the cell-cell contact areas increased between normal and Src cells as well as between adjacent Src cells, when Src cells were surrounded by normal cells (Fig. 6A,C). These increased cell-cell contact areas in Src cells were substantially reduced when Blebbistatin was added (Fig. 6A,C). Collectively, these results indicate that myosin-II induces basal localization of the E-cadherin–β-catenin complex, while enhancing cell-cell contact areas. The functional significance of this redistribution is not clear at present, but dynamic reassembly of the E-cadherin–β-catenin complex has been suggested to produce energy force and is often accompanied by morphological changes in an epithelial sheet, such as invagination (Kolsch et al., 2007; Oda et al., 1998). Thus, it is plausible that basal deviation of E-cadherin-based cell-cell adhesions is involved in promotion of apically directed movement of Src cells.

FAK functions upstream of MAPK in apical extrusion of Src cells

Src has been reported to phosphorylate several tyrosines in FAK (Calalb et al., 1995; Calalb et al., 1996; Schlaepfer and Hunter, 1996). After Src-mediated tyrosine phosphorylation, one of the tyrosine phosphorylation sites (Y925) of FAK binds to the Grb2-Sos complex, leading to activation of MAPK (Renshaw et al., 1999; Schlaepfer et al., 1994; Schlaepfer and Hunter, 1996). We found that PF573228, which blocks the kinase activity of FAK, significantly suppressed apical extrusion of Src cells from a monolayer of normal cells (Fig. 7A), suggesting that the activity of FAK is required for extrusion. We analysed the effect of Src activation on phosphorylation of FAK Y925 by immunofluorescence. When Src cells alone formed a monolayer, we observed enhanced phosphorylation of FAK Y925 at cell-cell and cell-matrix adhesion sites (Fig. 7B,C). Interestingly, when Src cells were surrounded by normal cells, phosphorylation of FAK Y925 was further enhanced around the whole cortex of the Src cells (Fig. 7B,C). Neither Blebbistatin nor U0126 affected the phosphorylation of FAK Y925 (Fig. 7D). PF573228 significantly suppressed the phosphorylation of MAPK in Src cells (Fig. 7F), but did not affect the phosphorylation of MLC (Fig. 7E). These results suggest that FAK functions upstream of MAPK.

We also found that addition of PF573228 significantly suppressed cell height of Src-transformed cells that were surrounded by normal cells (supplementary material Fig. S5A). In addition, PF573228 significantly blocked the relocalization of the E-cadherin–β-catenin complex in Src cells (supplementary material Fig. S5B). By contrast, addition of MEK inhibitor did not affect cell height or localization of the E-cadherin–β-catenin complex in Src cells (supplementary material Fig. S5A,B). These data indicate that FAK affects cell morphology and intercellular adhesions independently of MAPK. To further elucidate the function of FAK, we analysed tyrosine phosphorylation in Src cells. As shown in supplementary material Fig. S6A,B, tyrosine phosphorylation was strongly enhanced along the entire plasma membrane of Src cells, when they were surrounded by normal cells. This enhanced tyrosine phosphorylation was significantly suppressed in the presence of FAK inhibitor, but not in the presence of MEK inhibitor (supplementary material Fig. S6C), suggesting that FAK, but not MAPK, is involved in this process.

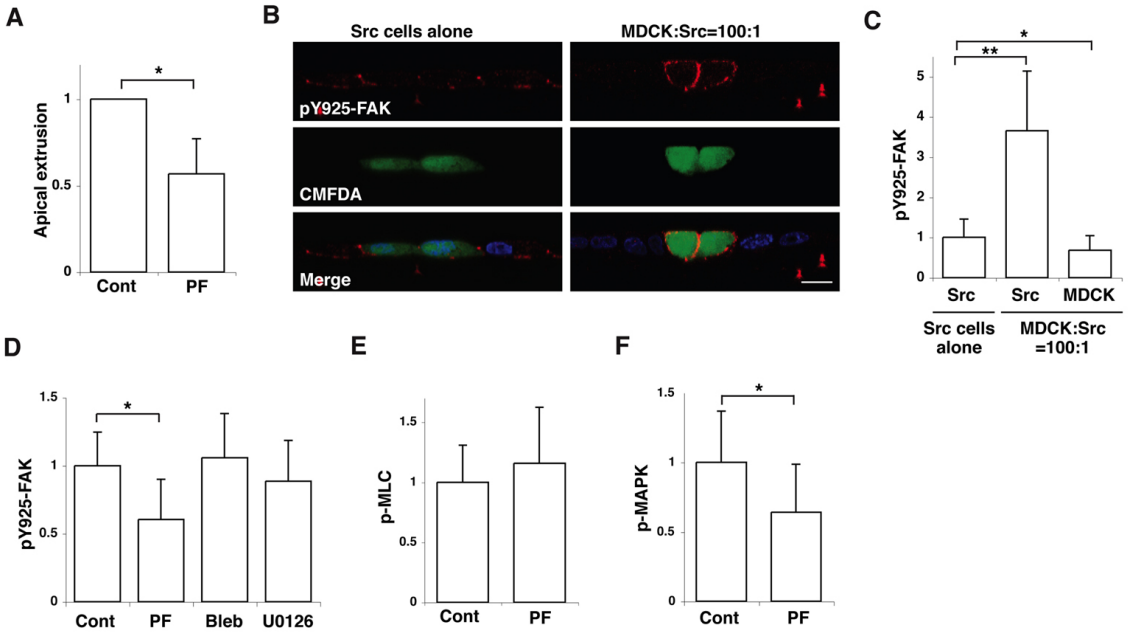

Fig. 7. FAK is involved in apical extrusion of Src cells. (**A**) Quantification of apical extrusion of ts-Src MDCK cells that are surrounded by normal MDCK cells in the absence or presence of PF573228 (PF). Data are mean ± s.d. from three independent experiments. **P*<0.02. (**B**) Immunofluorescence of XZ sections of Y925-*P* of FAK (pY925-FAK) in ts-Src MDCK cells (stained with CMFDA, green) surrounded by ts-Src MDCK cells (left panels) or by normal MDCK cells (right panels). Cells were stained with anti-Y925-*P*-FAK antibody (red) and Hoechst 33342 (blue). Scale bar: 10 µm. (**C**) Quantification of immunofluorescence of Y925-*P*-FAK in normal or Src cells. Data are mean ± s.d. **P*<2×10^{-6}, ***P*<1×10^{-32}; *n*=61, 59 and 59 cells from three independent experiments. (**D-F**) Quantification of immunofluorescence of Y925-*P*-FAK (D), MLC-*P* (E) or MAPK-*P* (F) in Src cells that are surrounded by normal cells in the absence or presence of inhibitors. Data are mean ± s.d. (D) **P*<0.0001, Z=6.1; *n*=55, 51, 65 and 39 cells from three independent experiments. (E) *n*=52 and 46 cells from three independent experiments. (F) **P*<0.0001, Z=4.7; *n*=54 and 53 cells from three independent experiments. Values are expressed as a ratio relative to control (A,D-F) or Src cells alone (C). Two-tailed Student's *t* tests were used to determine *P*-values, except for Fig. 7D,F where Mann-Whitney *U*-tests were used.

Phosphorylation of paxillin, a well-known substrate of FAK, was localized exclusively at the basal side of Src cells and was absent at the apical and lateral membrane domains (supplementary material Fig. S6D), suggesting there are other substrate(s) of FAK under this condition. It remains to be studied in future which proteins are phosphorylated by FAK and how phosphorylation of these proteins affects the signalling pathways and behaviour of Src cells that are surrounded by normal cells.

Discussion

In this study, we show that multiple signalling pathways become activated in Src-transformed MDCK cells when they are surrounded by normal MDCK cells, leading to apical extrusion of the transformed cells (Fig. 8). We have previously shown that RasV12-transformed cells are also apically extruded from a monolayer of normal epithelial cells (Hogan et al., 2009). Apical extrusions in these two systems share a number of features. First, apical extrusion occurs only when transformed cells are surrounded by normal cells. Second, the extrusion does not depend on apoptosis of the transformed cells. Third, the height of the transformed cells is increased when they are surrounded by normal cells. Fourth, myosin-II becomes activated in the transformed cells when they are surrounded by normal cells, and the myosin activity is involved in apical extrusion of the transformed cells. Fifth, MAPK activity is involved in apical extrusion of transformed cells. It is intriguing that the activation of Src or Ras, each of which regulates distinct signalling pathways, causes such similar responses. Indeed, our data in supplementary material Fig. S2B,C suggest that Ras and Src pathways play a role in apical extrusion of Src- and Ras-transformed cells, respectively. However, there is evidence to indicate that distinct signalling pathways are also regulated at the interface between normal and respective transformed cells. First, Ras-transformed cells that are not apically extruded form basal protrusions and invade the matrix (Hogan et al., 2009), whereas Src-transformed cells do not form similar protrusions (supplementary material Fig. S3). Second, when Src-transformed cells are surrounded by normal cells, activity of FAK is further enhanced, which is involved in apical extrusion (Fig. 7A-C). Third, when Src-transformed cells are surrounded by normal cells, tyrosine phosphorylation is strongly enhanced around the whole cortex of the Src cells, which is partially suppressed by the FAK inhibitor PF573228 (supplementary material Fig. S6A-C). Such enhanced tyrosine phosphorylation around the whole cell cortex is not observed in Ras-transformed cells (our unpublished observation). Fourth, when Src-transformed cells are surrounded by normal cells, phosphorylation of MAPK is observed around the entire plasma membrane of Src cells (Fig. 5C), whereas phosphorylation of MAPK is observed in the cytosol of Ras-transformed cells that are surrounded by normal cells (our unpublished observation), suggesting that distinct substrate proteins are phosphorylated by MAPK in the respective transformed cells. Collectively, these data demonstrate that there are some overlapping signalling pathways involved in apical extrusion of Src- and Ras-transformed cells, but that in addition, distinct signalling pathways are also regulated, which influence the behaviour and fate of the respective transformed cells.

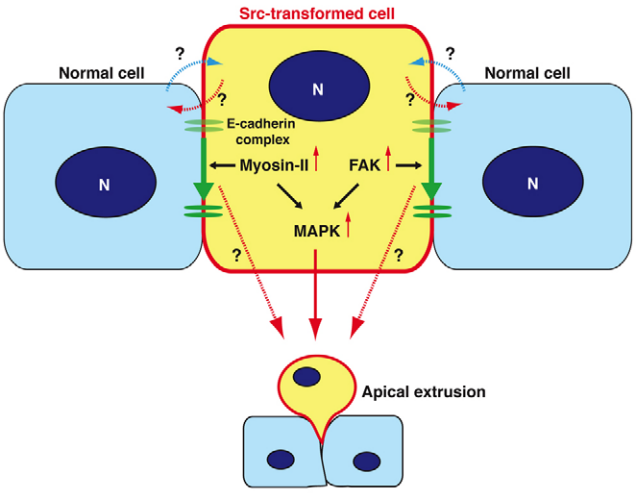

Fig. 8. Molecular mechanisms of apical extrusion of Src cells. In Src cells that are surrounded by normal cells, activity of myosin-II and FAK is increased, leading to activation of the downstream MAPK pathway. Activity of myosin-II, FAK and MAPK is involved in apical extrusion of Src cells. In addition, E-cadherin-based cell-cell adhesions are basally relocalized in a myosin-II- and FAK-dependent manner. N, nucleus.

Our data suggest that Src-transformed cells recognize that they are surrounded by normal cells and, in response, activate multiple intracellular signalling pathways. How do Src cells sense their untransformed neighbours? We demonstrate that a Gap junction inhibitor does not affect apical extrusion of Src cells (Fig. 4), suggesting that communication via Gap junctions is not involved in the intercellular recognition and/or the extrusion process. There is increasing evidence that cells are able to sense the physical properties, such as surface tension and elasticity, of their surroundings (Jaalouk and Lammerding, 2009; Orr et al., 2006; Vogel and Sheetz, 2006). Using atomic force microscopy (AFM), we have found that Src cells have higher elasticity than normal cells (data not shown). It remains to be elucidated whether these differences in elasticity contribute to the recognition process involved in the extrusion response.

In order to study the events occurring at the interface between normal and transformed cells, we have used inducible mammalian cell culture systems (Hogan et al., 2009), which allow us to analyse the differences between transformed cells surrounded by normal cells and those surrounded by transformed cells themselves. For this purpose, *Drosophila* is currently the most suitable in vivo system whereby genetic ablation can be induced in a mosaic manner or within the entire tissue. Indeed, in the *Drosophila* wing or eye disc epithelium, various non-cell-autonomous cellular processes have been shown to occur at the interface between normal and transformed cells (Brumby and Richardson, 2003; de la Cova et al., 2004; Hogan et al., 2009; Moreno and Basler, 2004; Vidal et al., 2006). However, in vertebrates, there are very few in vivo systems that can be applied to investigate this issue. In this study, we have used the outer epithelial layer of zebrafish gastrula embryos as an in vivo model and have generated an EVL-specific Gal4-driver line. By injecting the UAS-v-Src vector at the one- to two-cell stage, we have induced v-Src expression in a mosaic manner within the EVL epithelium. In order to clarify the molecular mechanisms of apical extrusion of v-Src-expressing cells in vivo, it will be necessary in future to establish a transgenic line expressing v-Src within the entire EVL. By comparing the v-Src expressing cells in these transgenic lines, we can examine whether and how the presence of surrounding non-transformed cells affects the behaviour of v-Src-transformed cells. Establishment of such in vivo systems will help us further investigate the interface between normal and transformed epithelial cells in vertebrates.

We find that Src-transformed cells are extruded apically in both in vitro and in vivo experiments. In the *Drosophila* wing disc, by contrast, Src-activated cells are extruded basally, not apically, and this basal extrusion requires the activation of the JNK signalling pathway in the Src-activated cells (Vidal et al., 2006). Conversely, a JNK inhibitor does not suppress apical extrusion of Src-transformed MDCK cells (data not shown), suggesting that apical extrusion in MDCK cells and basal extrusion in fly discs involve some distinct signalling pathways. A similar difference between vertebrate epithelial cells and *Drosophila* disc cells has also been reported in apoptosis-dependent cell extrusion. In vertebrate epithelia, apoptotic cells are apically extruded from the monolayer (Erman et al., 2009; Kim et al., 1996; Rosenblatt et al., 2001; Strater et al., 1995), whereas apoptotic cells are basally extruded from the *Drosophila* disc epithelium (Hanson et al., 2005; Moreno and Basler, 2004; Shen and Dahmann, 2005). It is intriguing that the direction of extrusion of apoptotic and Src-transformed cells has been differently evolved between vertebrates and fly.

What is the physiological significance of apical extrusion of Src-transformed cells? Generally, to metastasize into other tissues, transformed epithelial cells have to leave the basal surface of the epithelial monolayer and migrate through the underlying matrix. Thus, through apical extrusion, cells move into the direction opposite to that required for metastasis. After apical extrusion, cells would face physically and chemically harsh environments in vivo (e.g. flow of urine or stool). Moreover, we have observed, both in vitro and in vivo, that apically extruded vertebrate cells adhere weakly to the apical surface of the epithelial layer and often dissociate from it. It is plausible that apical extrusion is the process whereby transformed cells are eliminated from the body, and that it might have evolved as a protective mechanism against metastasis. Further studies of the mechanisms involved in the apical extrusion of transformed vertebrate cells could lead to a novel preventive or prophylactic treatment for cancers.

Materials and Methods

Plasmids, antibodies and materials

pSG-vSrc was previously described (Fujita et al., 2002). pEGFP-N1-MLC-AA was a gift from Hiroshi Hosoya (Hiroshima University, Japan). pPCI-mEGFP-HRas and pPCI-mEGFP-HRas-S17N were purchased from Addgene (Cambridge, MA).

Mouse anti-β-catenin and mouse anti-phospho-tyrosine antibodies were obtained from BD Biosciences (San Jose, CA). Rabbit anti-phospho-myosin light chain 2 (MLC-*P*; Thr18/Ser19), rabbit anti-phospho-FAK (Y925-*P*), rabbit anti-phospho-paxillin (Y118-*P*), and rabbit anti-Src antibodies were purchased from Cell Signaling Technology (Danvers, MA). Rabbit anti-phospho MAPK (MAPK-*P*) antibody was from Promega (Madison, WI). Mouse anti-GAPDH antibody was from Chemicon International (Hampshire, UK). Mouse anti-GFP antibody was from Roche Diagnostics (Mannheim, Germany). Alexa-Fluor-647- and Alexa-Fluor-568-conjugated secondary antibodies were from Invitrogen (Carlsbad, CA). For immunofluorescence, anti-β-catenin, anti-phospho-tyrosine and anti-MAPK-*P* antibodies were used at a dilution of 1:100, and anti-MLC-*P*, anti-Y925-*P* FAK and anti-Y118-*P* paxillin antibodies were used at 1:50. All secondary antibodies were used at 1:200. TRITC-phalloidin (Sigma-Aldrich, St Louis, MO) and Alexa-Fluor-647-conjugated phalloidin (Invitrogen) were used at 1.5 μg ml^{-1}. To visualize nuclei we used Hoechst 33342 (Invitrogen). For western blotting, all primary antibodies were used at a dilution of 1:1000.

To fluorescently stain living Src cells, CMTPX (red dye) or CMFDA (green dye) (Invitrogen) were used according to the manufacturer's instructions. To stain dead cells, plasma membrane-impermeable ethidium homodimer-1 (Invitrogen) was used

at 1 μM. Where indicated, the following inhibitors were used: 4-AP (2 mM, Sigma-Aldrich), (S)-(–)-Blebbistatin (30 μM, Toronto Research Chemicals, ON, Canada), U0126 (10 μM, Promega), PF573228 (20 μM, TOCRIS Bioscience, Ellisville, MO), and αGA (50 μM, Sigma-Aldrich). It should be noted that αGA has been reported to efficiently block gap junctions in MDCK cells (Abraham et al., 1999; De Blasio et al., 2004). LY294002, ML-7, and Y27632 were from Calbiochem (Darmstadt, Germany) and were all used at 10 μM. PP2 (Calbiochem) was used at indicated concentrations. All inhibitors were added for 14-24 hours incubation. Type-I collagen was obtained from Nitta Gelatin (Nitta Cellmatrix Type I-A, Osaka, Japan), and was neutralized according to the manufacturer's instructions.

Cell culture

MDCK cells, ts-Src MDCK, and HEK293 cells were cultured in Dulbecco's modified Eagle's medium (DMEM) supplemented with 10% fetal calf serum (FCS) and penicillin/streptomycin at 37°C for MDCK and HEK293 cells or at 40.5°C for ts-Src MDCK cells in ambient air supplemented with 5% CO_2. MDCK cells stably expressing GFP-RasV12 in a tetracycline-inducible manner were established and cultured as previously described (Hogan et al., 2009). For transient expression experiments, MDCK cells were seeded on collagen-coated coverslips in six-well culture dishes (Nunc, Roskilde, Denmark) at a density of 7×10^5 cells per well. On the following day, cells were transiently transfected with indicated constructs using Lipofectamine 2000 (Invitrogen) according to the manufacturer's protocol. For quantification of apical extrusion, cells were analysed after 28 hours of transfection.

Time-lapse analyses and immunofluorescence

ts-Src MDCK cells that were cultured at 40.5°C were fluorescently labelled, mixed with unlabelled normal MDCK cells or ts-Src MDCK cells at a ratio of 1:100, and seeded on the collagen matrix as previously described (Hogan et al., 2009). The mixture of cells was incubated for 7-8 hours at 40.5°C until a monolayer was formed. For time-lapse analyses, cells were observed at 35°C by Zeiss Axiovert 200M with a Ludl Electronic Products Biopoint Controller. Images were captured every 10 minutes for 24 hours and analysed using the Volocity software (Improvision). For immunofluorescence, the mixture of cells was incubated at 35°C for 14-16 hours for analyses of Src cells that remained in a monolayer or for 24 hours for analyses of apical extrusion.

Cells cultured on collagen were fixed with 4% paraformaldehyde (PFA) in PBS for 15 minutes, washed in PBS, and permeabilized in PBS containing 0.5% Triton X-100 for 15 minutes. For MAPK-*P* staining, cells were fixed with 10% formaldehyde in PBS for 30 minutes, washed in PBS, and permeabilized in –20°C methanol for 10 minutes on ice. Immunofluorescence was performed as previously described (Hogan et al., 2009). Stained cells were examined using a Leica TCS SPE confocal microscope and Leica Application Suite (LAS) software. Images were quantified using Metamorph 6.0 digital analysis software (Universal Imaging).

Embryo maintenance and generation of transgenic fish

The maintenance of fish and the collection of embryos were performed as described before (Westerfield, 2000). To generate an enveloping layer-specific Gal4-driver line, we employed the *Tol2* system (Kawakami et al., 2004). We transferred the *Tol2* sequences from the vector pT2KXIGΔin (Urasaki et al., 2006) into pBR322, and added a multi-cloning site to generate pBR-Tol2-MCS. About 5-kb-upstream sequences from the transcription starting point of the keratin 18 (*krt18*) gene were PCR-amplified based on a BAC (CH211-133J6; BACPAC Resources Center), and placed in front of the Gal4 DNA-binding domain fused with a synthetic activation sequence (Gal4FF) (Asakawa et al., 2008). Then, we transferred the krt18:Gal4 sequence to the vector pBR-Tol2-MSC, thus generating pBR-Tol2-krt18:Gal4. The resulting construct DNA (20 pg) was co-injected with 20 pg of RNA encoding *Tol2* into one-cell embryos carrying UAS:GAP43-GFP. The embryos exhibiting GFP expression at 24 hours post-fertilization (hpf) were raised to adulthood, and crossed with UAS:GAP43-GFP fish to identify founder fish. The founder fish were out-crossed with WT, and the F1 fish were selected for only Gal4 sequence, thus establishing the EVL:Gal4 line. All the embryos for experiments were obtained from crossing fish heterozygous for EVL:Gal4 with WT fish.

Microinjection and confocal imaging of zebrafish embryos

To follow cells expressing v-Src in zebrafish embryos, the self-cleaving 2A peptide sequence (SC) was used to bridge the GAP43-GFP and v-Src sequences (Szymczak et al., 2004). GAP43-GFP-SC-v-Src domain was then transferred into *Eco*RV/*Not*I sites of pBR-Tol2-UAS in which the UAS sequence and the E1B minimal promoter from pCS-5xUAS-EGFP (a gift from Masahiko Hibi, RIKEN CDB, Kobe) (Asakawa et al., 2008) was placed into pBR-Tol2-MCS. The Gal4-dependent expression of pBR-Tol2-UAS-GAP43-GFP-SC-v-Src was confirmed in HEK293 cells; pBR-Tol2-UAS-GAP43-GFP-SC-v-Src was transfected in HEK293 cells with or without pCS2-Gal4FF (a gift from Masahiko Hibi) (Asakawa et al., 2008), and cell lysates were analysed by western blotting. RNA encoding *Tol2* was synthesized by linearizing pCS2-TP (Kawakami et al., 2004), then transcribing with SP6 RNA polymerase essentially as described (Smith, 1993). Either GAP43-GFP or GAP43-GFP-SC-vSrc of the UAS-effecter DNAs (10-20 pg) was co-injected with 20 pg of *Tol2* RNA in EVL:Gal4 embryos at the one- to two-cell stage. The usage of the *Tol2* transposase system facilitates a transient integration of injected DNA, and reduces the toxicity due to DNA injection. The injected embryos were fixed in 4% PFA at 80-90% epiboly for whole-mount antibody staining. Whole-mount immunohistochemistry was performed as described previously with a minor modification (Shanmugalingam et al., 2000). Stained embryos were mounted in 0.8% low-melting agarose (Sigma-Aldrich) in embryo medium. Confocal images were taken using a 20× or 40× water-immersion lens on Leica DM2500 microscope with the TCS SPE confocal system. The XY and XZ projection images were produced using the Leica LAS software and Volocity software, respectively.

Data analyses

For data analyses, two-tailed Student's *t*-tests were used to determine *P*-values, except for Fig. 5F and Fig. 7D,F where Mann-Whitney *U*-tests were used. For quantification of apical extrusion or immunofluorescence intensity, one or two Src cells that were surrounded by normal or Src cells were analysed. For quantification of apical extrusion of Src cells using confocal microscopy (Fig. 1E,G, Fig. 4 and Fig. 7A; supplementary material Fig. S2B and Fig. S4), more than 40 Src cells were analysed for each experimental condition. For analyses of Src cells that remained in a monolayer, we analysed them after 14-16 hours of Src activation. At the time point, there were Src cells that were about to be extruded and had increased cell height and signalling pathways, but there were also some Src cells that had not yet responded to surrounding normal cells. Probably because of such a relatively heterogeneous response time of Src cells to the surrounding normal cells, the standard deviation was high in some of the results.

We thank Martin Raff for critical reading of the manuscript. We also thank Hiroshi Hosoya (Hiroshima University) and Masahiko Hibi (RIKEN CDB, Kobe) for constructs. Y.F. is supported by MRC funding to the Cell Biology Unit. M.T. is supported by MRC. G.C. is a Royal Society University Research Fellow. Deposited in PMC for release after 6 months.

Supplementary material available online at
http://jcs.biologists.org/cgi/content/full/123/2/171/DC1

References

Abraham, V., Chou, M. L., DeBolt, K. M. and Koval, M. (1999). Phenotypic control of gap junctional communication by cultured alveolar epithelial cells. *Am. J. Physiol.* **276**, L825-L834.

Asakawa, K., Suster, M. L., Mizusawa, K., Nagayoshi, S., Kotani, T., Urasaki, A., Kishimoto, Y., Hibi, M. and Kawakami, K. (2008). Genetic dissection of neural circuits by Tol2 transposon-mediated Gal4 gene and enhancer trapping in zebrafish. *Proc. Natl. Acad. Sci. USA* **105**, 1255-1260.

Baker, N. E. and Li, W. (2008). Cell competition and its possible relation to cancer. *Cancer Res.* **68**, 5505-5507.

Behrens, J., Vakaet, L., Friis, R., Winterhager, E., Van Roy, F., Mareel, M. M. and Birchmeier, W. (1993). Loss of epithelial differentiation and gain of invasiveness correlates with tyrosine phosphorylation of the E-cadherin/beta-catenin complex in cells transformed with a temperature-sensitive v-SRC gene. *J. Cell Biol.* **120**, 757-766.

Brumby, A. M. and Richardson, H. E. (2003). *scribble* mutants cooperate with oncogenic Ras or Notch to cause neoplastic overgrowth in Drosophila. *EMBO J.* **22**, 5769-5779.

Calalb, M. B., Polte, T. R. and Hanks, S. K. (1995). Tyrosine phosphorylation of focal adhesion kinase at sites in the catalytic domain regulates kinase activity: a role for Src family kinases. *Mol. Cell. Biol.* **15**, 954-963.

Calalb, M. B., Zhang, X., Polte, T. R. and Hanks, S. K. (1996). Focal adhesion kinase tyrosine-861 is a major site of phosphorylation by Src. *Biochem. Biophys. Res. Commun.* **228**, 662-668.

Carreira-Barbosa, F., Kajita, M., Morel, V., Wada, H., Okamoto, H., Martinez Arias, A., Fujita, Y., Wilson, S. W. and Tada, M. (2009). Flamingo regulates epiboly and convergence/extension movements through cell cohesive and signalling functions during zebrafish gastrulation. *Development* **136**, 383-392.

De Blasio, B. F., Rottingen, J. A., Sand, K. L., Giaever, I. and Iversen, J. G. (2004). Global, synchronous oscillations in cytosolic calcium and adherence in bradykinin-stimulated Madin-Darby canine kidney cells. *Acta Physiol. Scand.* **180**, 335-346.

de la Cova, C., Abril, M., Bellosta, P., Gallant, P. and Johnston, L. A. (2004). Drosophila myc regulates organ size by inducing cell competition. *Cell* **117**, 107-116.

Diaz, B. and Moreno, E. (2005). The competitive nature of cells. *Exp. Cell Res.* **306**, 317-322.

Erman, A., Zupancic, D. and Jezernik, K. (2009). Apoptosis and desquamation of urothelial cells in tissue remodeling during rat postnatal development. *J. Histochem. Cytochem.* **57**, 721-730.

Fagotto, F. and Gumbiner, B. M. (1996). Cell contact-dependent signaling. *Dev. Biol.* **180**, 445-454.

Fialkow, P. J. (1976). Clonal origin of human tumors. *Biochim. Biophys. Acta* **458**, 283-321.

Frame, M. C. (2002). Src in cancer: deregulation and consequences for cell behaviour. *Biochim. Biophys. Acta* **1602**, 114-130.

Frame, M. C., Fincham, V. J., Carragher, N. O. and Wyke, J. A. (2002). v-Src's hold over actin and cell adhesions. *Nat. Rev. Mol. Cell. Biol.* **3**, 233-245.

Fujita, Y., Krause, G., Scheffner, M., Zechner, D., Leddy, H. E., Behrens, J., Sommer, T. and Birchmeier, W. (2002). Hakai, a c-Cbl-like protein, ubiquitinates and induces endocytosis of the E-cadherin complex. *Nat. Cell Biol.* **4**, 222-231.

Hanahan, D. and Weinberg, R. A. (2000). The hallmarks of cancer. *Cell* **100**, 57-70.

Hanson, K. K., Kelley, A. C. and Bienz, M. (2005). Loss of Drosophila borealin causes polyploidy, delayed apoptosis and abnormal tissue development. *Development* **132**, 4777-4787.

Hogan, C., Dupre-Crochet, S., Norman, M., Kajita, M., Zimmermann, C., Pelling, A. E., Piddini, E., Baena-Lopez, L. A., Vincent, J. P., Itoh, Y. et al. (2009). Characterization of the interface between normal and transformed epithelial cells. *Nat. Cell Biol.* **11**, 460-467.

Hunter, T. and Sefton, B. M. (1980). Transforming gene product of Rous sarcoma virus phosphorylates tyrosine. *Proc. Natl. Acad. Sci. USA* **77**, 1311-1315.

Ikebe, M. and Hartshorne, D. J. (1985). Phosphorylation of smooth muscle myosin at two distinct sites by myosin light chain kinase. *J. Biol. Chem.* **260**, 10027-10031.

Jaalouk, D. E. and Lammerding, J. (2009). Mechanotransduction gone awry. *Nat. Rev. Mol. Cell. Biol.* **10**, 63-73.

Jamora, C. and Fuchs, E. (2002). Intercellular adhesion, signalling and the cytoskeleton. *Nat. Cell Biol.* **4**, E101-E108.

Kawakami, K., Takeda, H., Kawakami, N., Kobayashi, M., Matsuda, N. and Mishina, M. (2004). A transposon-mediated gene trap approach identifies developmentally regulated genes in zebrafish. *Dev. Cell* **7**, 133-144.

Kim, J., Cha, J. H., Tisher, C. C. and Madsen, K. M. (1996). Role of apoptotic and nonapoptotic cell death in removal of intercalated cells from developing rat kidney. *Am. J. Physiol.* **270**, F575-F592.

Kimura, K., Ito, M., Amano, M., Chihara, K., Fukata, Y., Nakafuku, M., Yamamori, B., Feng, J., Nakano, T., Okawa, K. et al. (1996). Regulation of myosin phosphatase by Rho and Rho-associated kinase (Rho-kinase). *Science* **273**, 245-248.

Kolsch, V., Seher, T., Fernandez-Ballester, G. J., Serrano, L. and Leptin, M. (2007). Control of Drosophila gastrulation by apical localization of adherens junctions and RhoGEF2. *Science* **315**, 384-386.

Koppen, M., Fernandez, B. G., Carvalho, L., Jacinto, A. and Heisenberg, C. P. (2006). Coordinated cell-shape changes control epithelial movement in zebrafish and Drosophila. *Development* **133**, 2671-2681.

Krendel, M. and Mooseker, M. S. (2005). Myosins: tails (and heads) of functional diversity. *Physiology (Bethesda)* **20**, 239-251.

Lecuit, T. and Lenne, P. F. (2007). Cell surface mechanics and the control of cell shape, tissue patterns and morphogenesis. *Nat. Rev. Mol. Cell. Biol.* **8**, 633-644.

Moreno, E. and Basler, K. (2004). dMyc transforms cells into super-competitors. *Cell* **117**, 117-129.

Nowell, P. C. (1976). The clonal evolution of tumor cell populations. *Science* **194**, 23-28.

Oda, H., Tsukita, S. and Takeichi, M. (1998). Dynamic behavior of the cadherin-based cell-cell adhesion system during Drosophila gastrulation. *Dev. Biol.* **203**, 435-450.

Orr, A. W., Helmke, B. P., Blackman, B. R. and Schwartz, M. A. (2006). Mechanisms of mechanotransduction. *Dev. Cell* **10**, 11-20.

Parsons, S. J. and Parsons, J. T. (2004). Src family kinases, key regulators of signal transduction. *Oncogene* **23**, 7906-7909.

Quintin, S., Gally, C. and Labouesse, M. (2008). Epithelial morphogenesis in embryos: asymmetries, motors and brakes. *Trends Genet.* **24**, 221-230.

Renshaw, M. W., Price, L. S. and Schwartz, M. A. (1999). Focal adhesion kinase mediates the integrin signaling requirement for growth factor activation of MAP kinase. *J. Cell Biol.* **147**, 611-618.

Rosenblatt, J., Raff, M. C. and Cramer, L. P. (2001). An epithelial cell destined for apoptosis signals its neighbors to extrude it by an actin- and myosin-dependent mechanism. *Curr. Biol.* **11**, 1847-1857.

Schlaepfer, D. D. and Hunter, T. (1996). Evidence for in vivo phosphorylation of the Grb2 SH2-domain binding site on focal adhesion kinase by Src-family protein-tyrosine kinases. *Mol. Cell. Biol.* **16**, 5623-5633.

Schlaepfer, D. D., Hanks, S. K., Hunter, T. and van der Geer, P. (1994). Integrin-mediated signal transduction linked to Ras pathway by GRB2 binding to focal adhesion kinase. *Nature* **372**, 786-791.

Shanmugalingam, S., Houart, C., Picker, A., Reifers, F., Macdonald, R., Barth, A., Griffin, K., Brand, M. and Wilson, S. W. (2000). Ace/Fgf8 is required for forebrain commissure formation and patterning of the telencephalon. *Development* **127**, 2549-2561.

Shen, J. and Dahmann, C. (2005). Extrusion of cells with inappropriate Dpp signaling from Drosophila wing disc epithelia. *Science* **307**, 1789-1790.

Smith, J. C. (1993). Purifying and assaying mesoderm-inducing factors from vertebrate embryos. In *Cellular Interactions in Development – A Practical Approach.* Oxford: Oxford University Press.

Strater, J., Koretz, K., Gunthert, A. R. and Moller, P. (1995). In situ detection of enterocytic apoptosis in normal colonic mucosa and in familial adenomatous polyposis. *Gut* **37**, 819-825.

Szymczak, A. L., Workman, C. J., Wang, Y., Vignali, K. M., Dilioglou, S., Vanin, E. F. and Vignali, D. A. (2004). Correction of multi-gene deficiency in vivo using a single 'self-cleaving' 2A peptide-based retroviral vector. *Nat. Biotechnol.* **22**, 589-594.

Urasaki, A., Morvan, G. and Kawakami, K. (2006). Functional dissection of the Tol2 transposable element identified the minimal cis-sequence and a highly repetitive sequence in the subterminal region essential for transposition. *Genetics* **174**, 639-649.

Vidal, M., Larson, D. E. and Cagan, R. L. (2006). Csk-deficient boundary cells are eliminated from normal Drosophila epithelia by exclusion, migration, and apoptosis. *Dev. Cell* **10**, 33-44.

Vogel, V. and Sheetz, M. (2006). Local force and geometry sensing regulate cell functions. *Nat. Rev. Mol. Cell. Biol.* **7**, 265-275.

Westerfield, M. (2000). *The Zebrafish Book*, 4th edn. Eugene: University of Oregon Press.

Woodcock, S. A., Rooney, C., Liontos, M., Connolly, Y., Zoumpourlis, V., Whetton, A. D., Gorgoulis, V. G. and Malliri, A. (2009). SRC-induced disassembly of adherens junctions requires localized phosphorylation and degradation of the rac activator tiam1. *Mol. Cell* **33**, 639-653.